

Controlling polar molecules in optical lattices

S. Kotochigova^{1,2} and E. Tiesinga¹

¹*Department of Physics, Temple University, Philadelphia, Pennsylvania 19122, USA*

²*National Institute of Standards and Technology, 100 Bureau Drive, Stop 8423, Gaithersburg, Maryland 20899, USA*

(Received 10 November 2005; published 17 April 2006)

We theoretically investigate the interaction of polar molecules with optical lattices and microwave fields. We demonstrate the existence of frequency windows in the optical domain where the complex internal structure of the molecule does not influence the trapping potential of the lattice. In such frequency windows the Franck-Condon factors are so small that near-resonant interaction of vibrational levels of the molecule with the lattice fields have a negligible contribution to the polarizability, and light-induced decoherences are kept to a minimum. In addition, we show that microwave fields can induce a tunable dipole-dipole interaction between ground-state rotationally symmetric ($J=0$) molecules. A combination of a carefully chosen lattice frequency and microwave-controlled interaction between molecules will enable trapping of polar molecules in a lattice and possibly realize molecular quantum logic gates. Our results are based on *ab initio* relativistic electronic structure calculations of the polar KRb and RbCs molecules combined with calculations of their rovibrational motion.

DOI: [10.1103/PhysRevA.73.041405](https://doi.org/10.1103/PhysRevA.73.041405)

PACS number(s): 33.80.Ps, 33.55.Be

Quantum gases of ultracold atoms and molecules, confined in periodic optical lattices, open exciting prospects for the ultimate control of their internal and external degrees of freedom. This control can be achieved by changing the intensity, wavelength, and geometry of the laser fields that create the lattice. Spectacular progress has been made in loading and manipulating atomic species in periodic optical potentials [1–5]. Theoretical developments have played an important role in this progress leading to a better fundamental understanding of observed phenomena and probing the possibility of using optical lattices in quantum computation with ultracold atoms [6,7].

Currently, the goal of many researchers is to perform similar experiments on cold molecular species. Optical lattices might be filled with ultracold molecules, which have been formed by photoassociation from ultracold colliding atoms [8–10] or, alternatively, be loaded with molecules cooled by deceleration [11] or thermalization with He [12]. Developments with trapped cold molecules have started a new field of physics [13].

Polar molecules are of particular interest in such experiments. This interest is based on the fact that polar molecules have a permanent dipole moment and therefore can interact via long-range dipole-dipole interactions. Trapped in an optical lattice the dipole-dipole interactions can make new types of highly correlated quantum many-body states possible [14]. Moreover, it has been proposed [15] that polar molecules trapped in an optical lattice can be good candidates for quantum bits of a scalable quantum computer. The electric dipole moment of ultracold polar molecules oriented by an external electric field may serve as the quantum bits and entanglement between qubits is due to the dipole-dipole interaction [16] between molecules. In principle, dipole moments can be induced in atoms and homonuclear molecules by external electric fields. For experimentally feasible static fields these induced dipole moments are weak, on the order of 10^{-2} D [17]. The permanent dipole moments in polar molecules are much larger, with typical values of 1 D.

In this Rapid Communication, we theoretically investigate the effects of optical lattice and microwave fields on polar molecules. The former are used to trap and the latter to align molecules. We start from ultracold polar molecules in the lowest rovibrational level of the ground electronic potential, possibly created by Raman photoassociation from its individual atoms. Moreover, we assume that there is one molecule per lattice site. Here we focus on KRb and RbCs polar molecules as they are proposed to be good candidates for ultracold experiments [18–20] and qubits of quantum information devices [15].

Localization of the molecule in a lattice site requires sufficiently deep lattice potentials, at least tens of kilohertz, to prevent tunneling of the molecule from one site to another. This can be achieved by increasing the laser intensity. On the other hand, higher laser intensities increase the possibility of exciting a molecule leading to unwanted decoherence processes. In particular, lattice fields of specific frequencies in the optical domain can transfer population from the lowest rovibrational level of the ground potential to a rovibrational level of an excited potential, which then by the spontaneous emission can decay to many rovibrational levels of the ground potential. As a result, we lose control over the molecule in the lattice. One of our goals is to determine lattice parameters that ensure strong trapping forces and simultaneously lead to small decoherence rates.

Controllable dipole-dipole interaction between polar molecules in a lattice lies at the heart of proposals to exploit entanglement as an essential resource for strongly correlated many-body states and quantum information processing. Even though polar molecules have a permanent electronic dipole moment, for any $J=0$ rotational state it averages to zero. Other rotational states ($J \geq 1$) do have a nonzero permanent dipole moment. In fact, for the $v=0$ level of the ground electronic state it is 0.76 D for KRb [21] and 1.27 D for RbCs [22]. We propose that a dipole moment is easily induced in a $J=0$ state by applying a microwave field with a

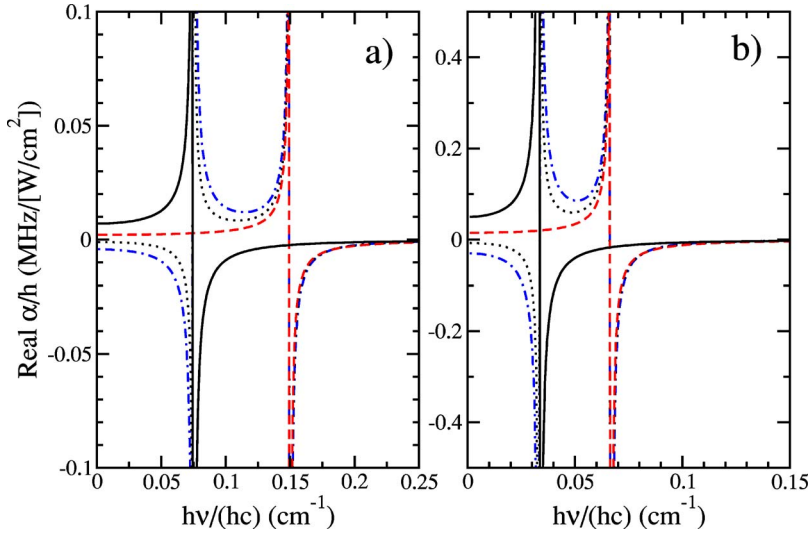


FIG. 1. (Color online) Dynamic polarizability for various photon polarizations of KRb (panel a) and RbCs (panel b) in the $J=0$ or $J=1$, $v=0$ rovibrational level of their $X^1\Sigma_0^+$ electronic ground state as a function of the microwave frequency. The solid line in both panels corresponds to the polarizability of the $J=0$ level, which is independent of the photon polarization. All other curves are for the $J=1$ level. The dotted line corresponds to the polarizability of $M=\pm 1$ magnetic sublevels illuminated by linear polarized σ_x or σ_y radiation. The dashed line relates to either $M=\pm 1$ sublevels illuminated by σ_z light or the $M=0$ level with σ_x or σ_y light. Finally, the dashed-dotted line is obtained for $M=0$ levels with σ_z light. Note that the scale on both axes differs for the two panels.

frequency that is close to the $J=0$ to $J=1$ resonance. Moreover, we investigate conditions under which the relevant states for a microwave transition have exactly the same ac Stark shift to minimize the field perturbations.

The relevant property for controlling a molecule with a light field is the complex molecular dynamic polarizability $\alpha(h\nu, \vec{\epsilon})$ as a function of radiation frequency ν and polarization $\vec{\epsilon}$ (h is the Planck constant). Assuming that the alkali-metal molecule is in a rovibrational state of the ground $X^1\Sigma^+$ potential, its dynamic polarizability in SI units is given in terms of the dipole coupling to other rovibrational states of the ground and excited potentials as

$$\alpha(h\nu, \vec{\epsilon}) = \frac{1}{\epsilon_0 c} \sum_f \frac{(E_f - ih\gamma_f/2 - E_i)}{(E_f - ih\gamma_f/2 - E_i)^2 - (h\nu)^2} |\langle f | d\hat{R} \cdot \vec{\epsilon} | i \rangle|^2, \quad (1)$$

where c is the speed of light, ϵ_0 is the electric constant, \hat{R} is the orientation of the interatomic axis, and i and f denote the initial $|vJM\rangle$ and intermediate $|v'J'M'\rangle$ rovibrational wave functions of the $|X^1\Sigma^+\rangle$ and $|\Omega\rangle$ electronic states, respectively. Ω labels either the $X^1\Sigma^+$ state or any excited state and $\langle f | d | i \rangle$ are R -dependent permanent or transition electronic dipole moments. The quantities M and M' are the projections along a laboratory fixed coordinate system of \vec{J} and \vec{J}' , respectively. The energy E_i is a rovibrational energy in the $X^1\Sigma^+$ state, and E_f is the rovibrational energy of the intermediate Ω states. Finally, the linewidths γ_f describe the spontaneous and any other decay mechanism that leads to loss of molecules. Equation (1) includes a sum over the dipole transitions to the rovibrational levels within the $X^1\Sigma^+$ potential as well as to the rovibrational levels of excited potentials. Contributions from scattering states or the continuum of the Ω states must also be included. The sum excludes the initial state. This sum, however, can be truncated, assuming that transitions may have zero or near zero electronic dipole moments and/or are far detuned. Nevertheless, a significant number of excited potentials and vibrational states have to be included.

The calculation of the molecular polarizability requires

the knowledge of molecular potential surfaces, permanent and transition dipole moments. We use data from our previous electronic structure calculations of KRb and RbCs polar molecules [21–23]. Here we combined them with nuclear dynamics calculations, based on a discrete variable representation [24], to obtain the rovibrational energies of and Franck-Condon factors between the ground and excited potentials of KRb and RbCs.

Our results for the molecular polarizability of KRb and RbCs at very-long wavelengths corresponding to microwave frequencies are shown in Fig. 1. Unlike the $J=0$ rotational level, the polarizability of $J \geq 1$ rotational levels depends on the polarization of light and the projection of \vec{J} . For microwave frequencies electric dipole transitions within the ground $X^1\Sigma^+$ potential dominate in the sum of Eq. (1). This $X^1\Sigma^+$ contribution does not exist for homonuclear molecules. The resonances in the graph are due to the rotational transitions from $J=0$ to $J=1$ and from $J=1$ to $J=0$ and $J=2$ within the same $v=0$ vibrational state. The $J=1$ to $J=2$ transition occurs at a larger photon frequency. For the near-resonance frequencies the polarizabilities in Fig. 1 are approaching $1 \text{ MHz}/(\text{W}/\text{cm}^2)$, which is much larger than atomic polarizabilities of K, Rb, and Cs in the same frequency region. For example, the dynamic polarizability of a Rb atom [25] is 4 to 5 orders of magnitude smaller than the dynamic polarizability of the RbCs molecule at the same frequency.

Figure 1 also shows that the $J=0$ and $J=1$ polarizabilities generally differ and even have opposite signs. However, although the vertical scale of the figure is too large to see this, for the $X^1\Sigma^+$ $v=0$ level they are the same at a frequency of $h\nu/(hc) \approx 0.3 \text{ cm}^{-1}$ for KRb and 0.1 cm^{-1} for RbCs. These might be so-called magic frequencies at which a microwave field creates the same ac Stark shift for a $J=0$ and a $J=1$ state. Our estimate shows that at the magic frequencies $\text{Re}(\alpha/h)$ equals $-0.5 \text{ kHz}/(\text{W}/\text{cm}^2)$ for KRb and $-3 \text{ kHz}/(\text{W}/\text{cm}^2)$ for RbCs.

For microwave fields nearly resonant with the $J=0$ to $J=1$ transition the $J=0$ molecular state is “dressed” and acquires a dipole moment. In fact, from perturbation theory the

strength of the induced dipole moment of the dressed $J=0$ state is

$$|\vec{d}_{\text{ind}}| \approx \left| 2 \frac{\langle\langle v,0 | -\vec{d} \cdot \vec{\mathcal{E}} | v,1 \rangle\rangle}{h\nu - (E_{X,v,J=1} - E_{X,v,J=0})} \langle\langle v,0 | \vec{d} | v,1 \rangle\rangle \right| \sim \sqrt{4\pi\epsilon_0} \frac{c}{2\pi} \alpha(h\nu, \vec{\epsilon}) \sqrt{I} \quad (2)$$

proportional to its polarizability. $|v, J\rangle = |X^1\Sigma^+\rangle |v, JM\rangle$, the energy $-\vec{d} \cdot \vec{\mathcal{E}}$ is the molecule-light coupling, $\vec{\mathcal{E}}$ is the applied electric field, and I is the corresponding intensity. The projection of the J state is determined by the polarization of the microwave field. Our estimates for the $v=0, J=0$ rovibrational level of RbCs indicate that in the limit of zero frequency, where $\text{Re}(\alpha/h) = 0.05 \text{ MHz}/(\text{W}/\text{cm}^2)$, and $I = 100 \text{ W}/\text{cm}^2$ the induced dipole moment is on the order of 0.05 times the permanent dipole moment, $\langle\langle v,1 | \vec{d} | v,1 \rangle\rangle$, of the $v=0, J=1$ level. At the magic microwave frequency a field intensity larger than $100 \text{ W}/\text{cm}^2$ is needed to achieve appreciable induced dipole moments.

For a microwave field resonant with the $J=0$ to $J=1$ transition, the dressed $J=0$ molecular state has an induced dipole moment of one half of the permanent dipole moment of the $v=0, J=1$ state. Assuming that $J=0$ polar molecules in neighboring lattice sites interact via tunable dipole-dipole forces $V_{dd} \sim d_{\text{ind}}^2/R_L^3$, where R_L is one half of a lattice wavelength, we can determine the characteristic interaction time $\delta t = h/V_{dd}$. If the lattice is made from laser light at optical frequencies, say at 690 nm for KRb or 810 nm for RbCs (we will justify this choice of frequencies later on), the interaction time for these molecules is as short as 2 ms. This time is short enough to establish entanglement of molecules during ultracold experiments with typical time scales of a few hundred milliseconds.

Light-induced decoherence of rovibrational levels of a polar molecule in the microwave region has two sources. The first source is spontaneous emission by electric dipole transitions to lower lying rovibrational levels. More important, however, is the decoherence due to black-body radiation from the room-temperature environment in the experiments. These two processes combined lead to lifetimes that are long ($\geq 100 \text{ s}$ as was shown in Refs. [22,23]) compared to currently realistic experimental time scales.

In the infrared and visible parts of the spectrum, molecules can be trapped in individual sites of the optical lattice. The depth of the lattice potential is determined by the real part of polarizability via $V_0 = -\text{Re} \alpha(h\nu, \vec{\epsilon}) \times I$, where I is the intensity of a field at frequency ν and polarization $\vec{\epsilon}$, while the laser-induced decoherence is proportional to the imaginary part of the polarizability. The left panel of Fig. 2 shows the potential energy curves of RbCs that are most relevant for and included in our calculation of the polarizability of rovibrational levels of the $X^1\Sigma^+$ state at these laser frequencies. The right panel shows the absolute value of the polarizability of the $v=0, J=0$ rovibrational level of the $X^1\Sigma^+$ state of RbCs. For infrared and optical domains, the dominant contribution to α is from rovibrational levels of the excited electronic potentials rather than from the ground state poten-

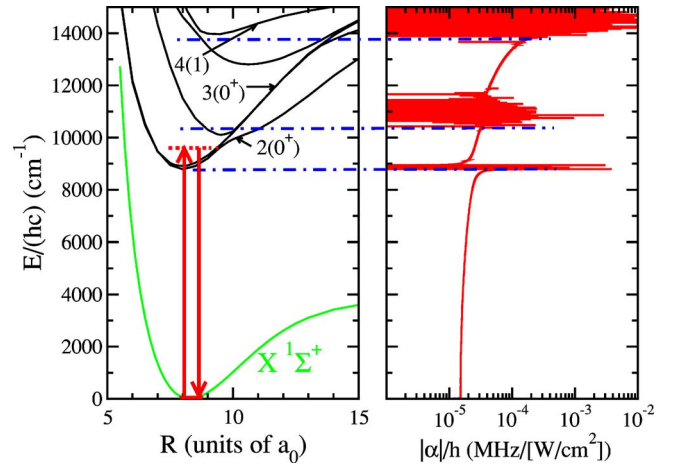


FIG. 2. (Color online) The ground and lowest excited potentials of RbCs as a function of internuclear separation (left panel) and the absolute value of the dynamic polarizability of the $v=0$ and $J=0$ level of the $X^1\Sigma^+$ electronic ground state as a function of laser frequency (right panel). The zero of energy of the left panel is the energy of the $v=0, J=0$ $X^1\Sigma^+$ level. The vertical axis of the two panels is the same. The two arrows illustrate a contribution to the dynamic polarizability. Three excited potentials with relativistic symmetry $\Omega^\pm=0^+$ have been labeled. The horizontal dashed lines correlate features in the polarizability with features in the potentials. (The polarizability is only evaluated at frequencies spaced by $h\Delta\nu/(hc)=1 \text{ cm}^{-1}$.)

tial. For KRb the potential energy curves and the polarizability have a similar structure.

Figure 2 shows that the polarizability has frequency windows where it is a slowly varying or “static” function interspersed with regions of multiple closely spaced resonantlike features, where α can be orders of magnitude larger. The resonantlike features are due to bound states of excited potentials and are closely related to inner- and outer-turning points of the excited potentials in the left panel of Fig. 2. The vibrational wave function of the $v=0, J=0$ $X^1\Sigma^+$ level is highly localized around the minimum of the $X^1\Sigma^+$ potential and, hence, a large vibrationally averaged transition dipole moment occurs when both the electronic dipole moment is large and excited vibrational levels have good overlap with the $v=0, J=0$ $X^1\Sigma^+$ level. Dashed-dotted horizontal lines in Fig. 2 make this connection between the two panels.

In the slowly varying regions of α above 9000 cm^{-1} there are hidden resonances that have negligible contribution to the polarizability due to small Franck-Condon factors with the ground state. For the figure, the polarizability is evaluated every $h\Delta\nu/(hc)=1 \text{ cm}^{-1}$ or $\Delta\nu=30 \text{ GHz}$, which is large compared to the vibrational level linewidths $\gamma \sim 6 \text{ MHz}$. This implies that if the vibrationally averaged transition dipole moment is large compared to or on the order of $h\Delta\nu$ a resonance appears in Fig. 2, while if it is small no resonance is visible.

Figure 3 shows both real and imaginary parts of the polarizability of the $v=0, J=0$ state of the $X^1\Sigma^+$ potential of KRb (upper panel) and RbCs (lower panel) in the optical domain. The imaginary part is proportional to the linewidth of the excited states and is smaller than the real part of the

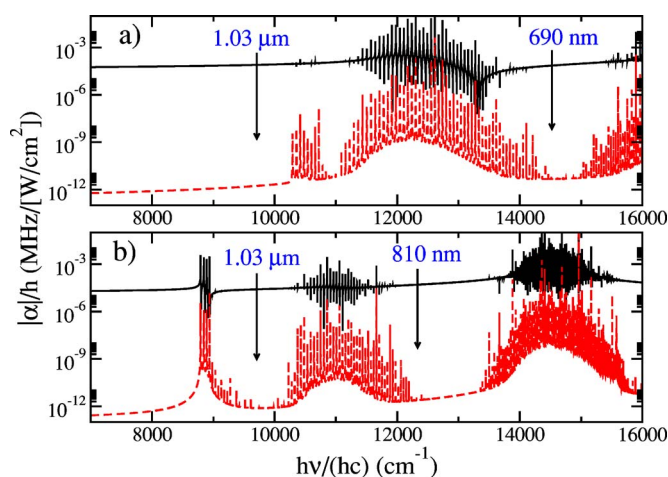


FIG. 3. (Color online) Real (solid line) and imaginary parts (dashed line) of the dynamic polarizability of the $v=0, J=0$ level of the $X^1\Sigma^+$ state of KRb (panel a) and RbCs (panel b) as a function of laser frequency. Practical laser frequencies are indicated.

polarizability for both molecules. In fact, the ratio between the real and imaginary parts of the polarizability is about 10^7 away from the resonances and significantly smaller ($\sim 10^3$) near them. Optical potentials seen by KRb or RbCs molecules in these regions can be very deep ($V_0/h \approx 1$ MHz) for laser intensities on the order of 10^4 W/cm 2 . At such intensities tunneling of molecules from one lattice site to another is

negligible. Moreover, the decoherence time is significantly larger than 1 s.

Using our results we propose two frequency intervals in which resonant excitation is unlikely and are most easy to work with experimentally. For the lattices in an optical domain, we suggest lasers with wavelengths between 680 ± 35 nm for a KRb and 790 ± 40 nm for a RbCs experiment. In addition, telecommunication wavelengths between 1.03 ± 0.05 μm seem practical for both molecules.

We conclude by saying that despite the fact that molecules have an internal structure that is more complex than atoms, this complexity can be used to good advantage or neutralized. Microwave fields nearly resonant with rotational transitions within the molecule can lead to tunable interactions between neighboring molecules. For optical lattice potentials created by standing light waves, a careful selection of laser frequency, in regions where the Franck-Condon factors to excited vibrational levels are small, creates conditions for which the ratio of coherent to decoherent effects is large and nearly independent on the internal molecular structure. Moreover, heavy polar alkali-metal molecules can be strongly confined in an optical lattice with relatively modest intensities.

The work was supported in part by the U.S. Army Research Office. We thank Dr. J. V. Porto and Professor D. DeMille and Professor S. L. Rolston for useful discussions.

- [1] D. R. Meacher, *Contemp. Phys.* **39**, 329 (1998).
 [2] M. Greiner *et al.*, *Nature (London)* **415**, 39 (2002).
 [3] G. Grynberg and C. Robilliard, *Phys. Rep.* **355**, 335 (2001).
 [4] C. Monroe, *Nature (London)* **416**, 238 (2002).
 [5] I. Bloch, *Nat. Phys.* **1**, 23 (2005).
 [6] P. S. Jessen and I. H. Deutsch, *Adv. At., Mol., Opt. Phys.* **37**, 95 (1996).
 [7] D. Jaksch H. J. Briegel, J. I. Cirac, C. W. Gardiner, and P. Zoller, *Phys. Rev. Lett.* **82**, 1975 (1999); *Phys. Rev. Lett.* **85**, 2208 (2000).
 [8] Y. B. Band and P. S. Julienne, *Phys. Rev. A* **51**, R4317 (1995).
 [9] R. Wynar *et al.*, *Science* **287**, 1016 (2000).
 [10] T. Rom *et al.*, *Phys. Rev. Lett.* **93**, 073002 (2004).
 [11] J. van Veldhoven *et al.*, *Eur. Phys. J. D* **31**, 337 (2004); E. R. Hudson *et al.*, *Eur. Phys. J. D* **31**, 351 (2004).
 [12] D. Egorov *et al.*, *Eur. Phys. J. D* **31**, 307 (2004).
 [13] Special issue of *Eur. Phys. J. D* **31**, 149 (2004), edited by J. Doyle, B. Friedrich, R. V. Krems and F. Masnou-Sseeuws.
 [14] B. Damski *et al.*, *Phys. Rev. Lett.* **90**, 110401 (2003).
 [15] D. DeMille, *Phys. Rev. Lett.* **88**, 067901 (2002).
 [16] R. Raussendorf and H. J. Briegel, *Phys. Rev. Lett.* **86**, 5188 (2001).
 [17] C. H. Townes and A. L. Shawlow, *Microwave Spectroscopy* (McGraw-Hill, New York, 1955), pp. 270–273.
 [18] H. Wang and W. C. Stwalley, *J. Chem. Phys.* **108**, 5767 (1998).
 [19] D. DeMille, D. R. Glenn, and J. Petricka, *Eur. Phys. J. D* **31**, 375 (2004).
 [20] A. J. Kerman, J. M. Sage, S. Sainis, T. Bergeman, and D. DeMille, *Phys. Rev. Lett.* **92**, 033004 (2004); A. J. Kerman, J. M. Sage, S. Sainis, T. Bergeman, and D. DeMille, *Phys. Rev. Lett.* **92**, 153001 (2004).
 [21] S. Kotochigova, P. S. Julienne, and E. Tiesinga, *Phys. Rev. A* **68**, 022501 (2003).
 [22] S. Kotochigova and E. Tiesinga, *J. Chem. Phys.* **123**, 1 (2005).
 [23] S. Kotochigova, E. Tiesinga, and P. S. Julienne, *Eur. Phys. J. D* **31**, 189 (2004).
 [24] E. Tiesinga, S. Kotochigova, and P. S. Julienne, *Phys. Rev. A* **65**, 042722 (2002).
 [25] M. S. Safronova, C. J. Williams, and C. W. Clark, *Phys. Rev. A*, **67**, 040303(R) (2003).